ASM Sc. J., 17, 2022

https://doi.org/10.32802/asmscj.2022.1093

# Influence on Ratio of NaOH/ZrSiO4 in Alkali Fusion for Amang Zircon Sand

I. Subuki[1,2*], N.F.F. Norsham[1], N.A. Mahayuddin[1] and Q.M. Ali[1]

[1]*School of Chemical Engineering, College of Engineering, Universiti Teknologi MARA, 40450 Shah Alam, Selangor, Malaysia*

[2]*Circular + Industrial Research Laboratory, School of Chemical Engineering, College of Engineering, Universiti Teknologi MARA, 40450 Shah Alam, Selangor, Malaysia*

Amang Zircon Sand from Amang Onn Sdn. Bhd. mineral company has a high composition of zirconium at 61.63 wt% and low silicon composition at 4.90 wt%. The high composition of zirconium in Amang zircon sand indicates the possibility to synthesise it into a zirconia. Zirconium was synthesised using alkali fusion method with different ratio of NaOH/ZrSiO4 to determine the optimum ratio based on the zirconium yield. Alkali fusion method is coupled with thermal treatment as it will produce a higher yield of zirconium with lower impurities. Then it will be leached with deionised water and hydrochloric acid (HCl). The synthesised zirconium was characterised through X-Ray fluorescence (XRF) spectroscopy, X-Ray diffraction (XRD) and particle size distribution (PSD) analysis. The XRF analysis after the fusion and thermal treatment shows a high composition of zirconium as well as great reduction of silicon. 1.2NaOH/ZrSiO4 is determined to be the optimum ratio as it has the lowest silicon impurity of 2.11 wt% and high yield of zirconium at 71.40 wt%. The low impurities will reduce the chance of cracking and maximising the efficiency of zirconia. It is supported by XRD patterns that are dominated by high zirconium peaks. The zirconium oxychloride obtained after acid leaching has a high zirconium composition. This shows that it is possible to use Amang zircon sand as a precursor to synthesis a zirconia using alkali fusion method with sodium hydroxide.

**Keywords:** Amang zircon sand; zircon sand; alkali fusion; zirconium; sodium hyrdoxide

## I. INTRODUCTION

Zircon sand with the chemical formula of $ZrSiO_4$ or also known as zirconium silicate usually contains traces of other elements such as zirconium dioxide ($ZrO_2$), silicon dioxide ($SiO_2$), titanium dioxide ($TiO_2$) and iron (III) oxide ($Fe_2O_3$) (Das & Bandyopadhyay, 2004; Pawłowski, Blanchart & Blanchart, 2018). This makes zircon sand as a great and inexpensive source of zirconium. It is a non-magnetic material and referred to as a heavy metal since zircon has a higher specific gravity (SG) of 4.6-4.7 (Hamzah, Ahmad & Saat, 2009). The specific gravity of zircon is higher due to the existence of heavy minerals in it (Kittiauchawal *et al.*, 2012).

Zircon is somehow attractive due to the chemical stability, high thermal decomposition temperature, resistance to erosion, high strength, toughness, high hardness, high stability, inert and biocompatibility and high ionic conductivity at high temperatures (Shi *et. al.*, 2012; Septawendar *et. al.*, 2016; Musyarofah *et al.*, 2019). Hence, it is widely used in various applications such as in the biomedical industry, polycrystal ceramic, foundry, catalyst, gas sensor and refractory (Van Tuyen *et. al.*, 2007; Hidalgo *et. al.*, 2013; Gauna *et. al.*, 2015; Atkinson, Mocioiu & Anghel, 2021). Furthermore, it can also be used for immobilisation of nuclear waste and as an additive in whitening agents in glaze (Li *et. al.*, 2022; Morfino *et al.*, 2022).

* Corresponding author's e-mail: istikamah@uitm.edu.my

It naturally exists as a form of sand from a by-product of weathered rocks and other deposits. It can also occur as an industrial by-product from earth compound extraction and tin mining process (Kumar *et. al.*, 2015; Abdullah *et al.*, 2022). Amang zircon sand, a by-product of a rough concentration of casserite (tin dioxide) that is typically dark brown in colour can be obtained in tin mining process with valuable heavy minerals such as ilmenite, monazite, xenotime and zircon (Azreen *et. al.*, 2018; Sanusi *et al.*, 2021).

The usage of Amang zircon sand helps to reduce the by-product that is typically abandoned after the mining process especially after the decreasing demand in global market (Abdullah *et al.*, 2022). It is also an inexpensive source. However, all undesired elements that exist in zircon such as iron, aluminium, silicon, nickel and titanium must be removed before it can be used as a raw material for zirconia as it will affect the zircon decomposition and efficiency of zirconia (Yang *et al.*, 2021).

There are various techniques available to synthesise zirconium from zircon such as sol-gel method, alkali fusion with caustic soda (NaOH), hydrothermal, microwave plasma synthesis, and mechanochemical treatment (Keiteb *et. al.*, 2017; Ebrahimi, Hamidi & Pourabdoli, 2022). However, the most commonly used method in the industry is alkali fusion with sodium hydroxide because it promotes the efficiency of impurity removal from the zircon sand, increases the rate of zircon decomposition and the product can be altered in accordance to the application needed (Biswas *et. al.*, 2010; Septawendar *et al.*, 2016). This fusion of zircon can also be used in a larger production scale of zirconia because of the low sintering temperature and time which results to a low operational cost compared to other methods.

According to previous research, decomposition of zircon by using NaOH works best in ratio of 1.2 and 1.7 (Abdelkader, Daher & El-Kashef, 2008). In fact, a higher mass ratio of NaOH/ZrSiO4 will increase the conversion of zircon to zirconium (Da Silva, Dutra & Afonso, 2012). However, using a higher percentage of NaOH than recommended will result in the formation of sodium zirconium oxide silicate ($Na_2ZrSiO_5$) which is water insoluble and needs to be dissolved in acid. It will also increase the silicon composition after acid leaching process as this compound is bound to dissociate in acid, hindering the formation of zirconium. Higher zirconium recovery and low silicon production can be achieved if an optimum ratio of NaOH/ ZrSiO4 is discovered. Therefore, investigating the influence on ratio of $NaOH/ZrSiO_4$ in alkali fusion method for Amang zircon sand is necessary.

## II. METHODOLOGY

### *A. Materials*

Amang Zircon Sand from Amang Onn Sdn. Bhd. mineral company in Kampar, Perak is used as received. Solid sodium hydroxide (NaOH) and analytical grade of hydrochloric acid (HCl) from R&M Chemicals are used to synthesise zirconium from zircon sand and deionised water (DI-H20) is used as a water leaching agent.

X-Ray fluorescence (XRF) spectroscopy is conducted to evaluate the chemical composition of zirconium in zircon sand using PANanalytical Axios-Max, Netherlands. X-ray diffraction (XRD) from Philips PANanalytical E'Pert Pro PW 3040, Netherlands, using Cu Kα radiation source with a wavelength (λ) of 0.15 nm, scanning range of 10-80° at 40 kV and 35 mA setting. The scanning rate is set at 2°/minute and step size of 0.02°. Particle size distribution (PSD) analysis is done using Mastersizer 2000, Malvern, Britain, to determine the particle size and particle width distribution.

### *B. Method*

Zirconium is studied by using alkali fusion method. The alkali fusion technology is presented in Figure 1. Zircon sand is mixed with sodium hydroxide (NaOH) or caustic soda in an iron crucible to produce sodium compounds of sodium zirconate and sodium orthosilicate (Sun *et al.,* 2019). The process is done in accordance to Equation (1):

$$ZrSiO_4 + 6NaOH \rightarrow Na_2ZrO_3 + Na_4SiO_4 + 3H_2O \quad (1)$$

A variation of ratio of sodium hydroxide (NaOH) ranging from 1.2, 1.3 and 1.5 were applied in order to study the effect of $NaOH/ZrSiO_4$ ratio on zircon decomposition. A thermal treatment is then conducted following the alkali fusion reaction. The treatment is done by using a constant heating rate of 20 °C/min. The temperature was set up to 100 °C, and then 200 °C and held for 1 hour respectively before the

temperature was increased to 670 °C. This temperature is then held for 2 hours.

After the thermal treatment, the powdery caustic frit existed in two phases which are inorganic water-soluble sodium silicate ($Na_2SiO_3$) and water insoluble sodium zirconate ($Na_2O_3Zr$) (Abdelkader, Daher & El-Kashef, 2008). The reactions involved are:

$$Na_2ZrO_3 + Na_2Si_2O_5 \rightarrow Na_2ZrO_3 + Na_2SiO_3 \quad (2)$$

$$Na_4SiO_4 + ZrSiO_4 \rightarrow Na_2ZrSiO_5 + Na_2SiO_3 \quad (3)$$

The frits from varied ratio of $NaOH/ZrSiO_4$ are analysed in order to determine the highest zirconium recovery. The frit from the optimum ratio is then leached five times with deionised water using a ratio of 1:8 in order to remove excess NaOH, unreacted zircon and sodium silicate using Equation (4):

$$Na_2ZrO_3 + 2H_2O \rightarrow ZrO(OH)_2 + 2NaOH \quad (4)$$

The solid sodium zirconate is filtrated from liquid sodium silicate using filter paper (Liu *et al.*, 2014). The sodium zirconate cake is then leached with hydrochloric acid (HCl) to precipitate silicate using Equation (5):

$$Na_2ZrO_3 + 4HCl \rightarrow ZrOCl_2 + 2NaCl + 2H_2O \quad (5)$$

It is then left for at least 1 hour to obtain zirconium oxychloride with excess sodium silicate. The excess sodium silicate is filtered using filter paper to obtain pure zirconium oxychloride or zirconyl chloride ($ZrOCl_2$). The zirconium oxychloride is then dried at room temperature for 24 hours. Samples are analysed to determine the effectiveness of sodium hydroxide in decomposing zircon to zirconium using alkali fusion method.

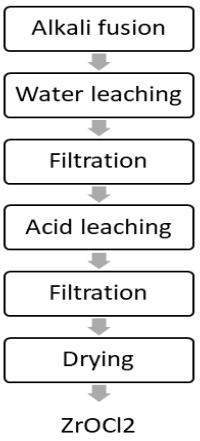


Figure 1. Alkali fusion technology of Amang zircon sand

## III. RESULTS AND DISCUSSION

### *A. Chemical Composition*

The composition of raw Amang zircon sand before alkali fusion can be seen in the X-Ray fluorescence analysis in Table 1. 61.63 wt% of zirconium (Zr) is recorded in the raw Amang zircon sand which is slightly lower compared to other studies done previously with zircon sand from West Borneo, Indonesia and Beijing, China (Septawendar *et. al.*, 2016; Sun *et al.*, 2019). This analysis showed that zirconium was the major element in Amang zircon sand. Zircon sand also consist of impurities such as silicon (Si) and hafnium (Hf) which are recorded at 4.90 wt% and 1.43 wt%, respectively. These amounts are considered as staggeringly low. This is comparable to the research by Musyarofah *et al.* (2019) concerning the presence of silicon, hafnium and ferum in zircon sand. Besides, titanium was found together with zircon in the form of rutile, ilmenite and leucoxene (Attallah, Hilal & Moussa, 2017). This further validate the chemical composition analysis of raw Amang zircon sand. The low composition of impurities in Amang zircon sand might be due to the magnetic separation process that was done by the company. Magnetic separation process enhanced the recovery of zirconium by removing the magnetic impurities in the zircon sand (Murti *et al.*, 2019).

Other impurities such as magnesium (Mg), potassium (K), gallium (Ga), arsenic (As), ytterbium (Yb), lead (Pb) and bismuth (Bi) are also recorded to be at 28.87 wt% in total. Based on the analysis, Amang zircon sand has other elements such as cerium (Ce), thorium (Th), and neodymium (Nd). The presence of radionuclides such as thorium in Amang zircon

sand is in accordance to the report by Ismail *et al.* (2001). This is due to the monazite minerals in the zircon sand. However, the amount of thorium found in the Amang zircon sand is considered to be low to trigger any radioprotection standard.

The major element in zircon sand which is zirconium showed an increment in composition after alkali fusion. The highest zirconium composition obtained after alkali fusion and thermal treatment was recorded at 72.66 wt% with a $NaOH/ZrSiO_4$ ratio of 1.3. This is because the decomposition reaction was increased by the higher NaOH content in the reaction (Sun *et al.*, 2019). Both ratios of 1.2 and 1.3 showed a positive increment of zirconium composition. However, the composition of zirconium reduced to 68.38wt% when the ratio is changed to 1.5 which suggests incomplete decomposition of zircon sand. This might be due to the high ratio of NaOH in which correlates to the high viscosity of NaOH. A higher viscosity of NaOH reduced the efficiency of the fusion by hindering the mass transfer and reacted with zircon sand at a less wettable condition in which resulted in a segregation (Mohammed & Daher, 2002; Chen & Bonaccurso, 2014; Liu *et al.*, 2016). Thus, incomplete decomposition occurred.

It is clearly shown that the zirconium composition of Amang zircon sand has a positive increase from raw until 1.3 ratio of $NaOH/ZrSiO_4$. However, the composition of zirconium linearly decreased once the ratio hits 1.5. This shows that $NaOH/ZrSiO_4$ ratio used for Amang zircon sand should not exceed 1.3 in order to improve the yield of zirconium during the alkali fusion process.

In addition, half of the silicon composition was removed after the fusion and thermal treatment. Silicon composition in the sample must be reduced as much as possible. This is important because it is actively formed during the reactions. Higher impurities increase the probability of cracking which will reduce the efficiency of zirconia synthesised from Amang zircon sand (Daou, 2014). Therefore, a 1.2 ratio is deemed as the optimum ratio of $NaOH/ZrSiO_4$ because it has high yield of zirconium with lowest silicon composition which is only at 2.11 wt%.

The thermal treatment was done in three steps in order to allow the decomposition reaction to start at a lower temperature before the temperature was raised. This method will utilise the fusion of zircon sand with NaOH before it reaches the melting point at 323 °C. The increased amount of zirconium after the fusion suggest a rapid decomposition occurred at 670 °C.

However, valuable heavy minerals such as biotite, garnet, ilmenite, magnetite, kyanite, monazite, xenotime in Amang zircon sand might also reduce the effectiveness of zircon decomposition (Biswas *et al.*, 2010). Unwanted impurities such as lanthanum and praseodymium elements were present in the $NaOH/ZrSiO_4$ with a ratio of 1.3 and 1.5 because of the monazite conversion in zircon sand. The increased amount of sodium hydroxide ratio can lead to the formation of lanthanum while the formation of praseodymium occurred after alkali fusion because of cerium and neodymium. This further proves that 1.2 is the most suitable ratio of $NaOH/ZrSiO_4$. Besides, the increased of NaOH will also produce a coarser frit that will adhere to the crucible making it difficult to remove from the crucible (Abdelkader, Daher & El-Kashef, 2008). These issues will make the procedure even more complicated as milling process is necessary and it will hinder the heat transformation between the reactants.

A fused mass of sodium zirconate, sodium silicate, unreacted sodium hydroxide, unreacted zircon and impurities were produced from the fusion of 1.2 $NaOH/ZrSiO_4$ as accordance to Equation (2) and (3) (Abdel-Rehim, 2005; Abdelkader, Daher & El-Kashef, 2008). The sodium silicate was leached out by the water due to its water-soluble property (Abdelkareem, 2019). This process is crucial as the hydrolysis of $Na_2ZrO_3$ can be hindered and subsequently decreasing the zirconium formation. The residues from water leaching consist of the insoluble sodium zirconate, hydrous zirconia from $Na_2ZrO_3$ hydrolysis, sodium silicate that was not completely removed from water leaching, unreacted zircon and other impurities (El Barawy, El Tawil & Francis, 2000). These residues will then be removed by acid leaching with hydrochloric acid (HCl). The compositions of the insoluble solid residue after acid leaching can also be seen in Table 1. Based on the chemical composition, the zirconium recovery was recorded at 67.14 wt% with a relatively low silicon composition at 2.46 wt%. The zirconium content was slightly low probably because $Na^+$ in the interlayer of $Na_2ZrO_3$ was not completely removed during the water leaching

process, thus, hindering the formation of $Na_2ZrO_3$ into zirconium oxychloride. At the end of the leaching process, the residue turned into a gel precipitate which indicated the formation of sodium silicate. A high temperature of 100 °C was used because formation of silica gel is highly favoured in high temperature and high concentration of HCl.

Zirconium oxychloride ($ZrOCl_2$) with excess sodium silicate were obtained when the gelatinous precipitate was dried. The slight increase in silicon composition is due to the formation of sodium silicate during the reaction. The remaining presence of $Na_2SiO_3$ dissolved and hydrolysed into $SiO_2$ after the acid treatment. According to Septawendar *et al.* (2016), the increased amount of silicon could be reduced by enhancing the process with water until the soluble sodium silicate is removed from zirconium oxychloride. Conversely, it can also be reduced by aging process in order to achieve a complete separation of silicate (Mohammed & Daher, 2002). Besides, titanium (Ti) could completely dissolved in the hot HCl if the raw sand undergoes ball milling process.

Table 1. Composition (wt%) of Amang zircon sand

| Element | Raw Amang | 1.2NaOH | 1.3NaOH | 1.4NaOH | Acid |
|---|---|---|---|---|---|
| Zr | 61.63 | 71.4 | 72.66 | 68.38 | 67.14 |
| Si | 4.90 | 2.11 | 2.41 | 2.42 | 2.46 |
| Hf | 1.43 | 1.76 | 1.90 | 1.74 | 1.73 |
| Ti | 1.13 | 1.21 | - | 1.36 | 1.55 |
| Fe | 0.17 | 0.11 | 0.17 | 0.19 | 0.21 |
| Ce | 0.55 | 3.74 | 5.54 | 5.53 | 4.92 |
| Ag | 0.42 | 0.41 | 0.44 | 0.51 | 0.42 |
| Y | 0.14 | 0.19 | 0.19 | 0.19 | 0.17 |
| Th | 0.20 | 0.62 | 0.99 | 1.65 | 0.98 |
| La | - | - | 2.74 | 2.95 | - |
| Nd | 0.16 | 1.15 | 1.67 | 1.97 | 1.40 |

### *B. Crystallisation*

The diffraction pattern can be seen in Figure 2 and the phase identification was done. The diffraction pattern of raw Amang zircon sand showed several sharp peaks which are unique to zircon. The main crystalline phase is determined to be zirconium silicate, $ZrSiO_4$ (ICDD 00-006-0266). A similar XRD pattern was observed by Genoveva *et al.* (2007). Most of the peaks are consistent with zirconium and silicon. For the raw Amang zircon sand, the highest peak was detected at 26.98° which is indicative to monoclinic zirconium dioxide ($ZrO_2$) (ICDD 00-002-0464). Quartz which is also known as silicon dioxide ($SiO_2$) is also detected at the highest peak (ICDD 01-0850794). This data supports the composition analysis by XRF which showed zirconium and silicon as the main and second elements, respectively in Amang zircon sand. The diffraction of raw Amang zircon also shows traces of impurities, rare earth elements and several other transition elements.

Based on the phase identification, zirconium can be detected at peaks 35.55°, 55.40°, 55.64°, 68.83°, 75.38° and 76.12° in the raw Amang (ICDD 00-024-1165). Often, silicon can be detected at nearby peak for example at 56.40° (ICDD 00-001-0791). This is due to the small composition of silicon as detected in XRF analysis. The same goes to rutile which is also known as $TiO_2$. A very small presence of rutile can be detected in some minor peaks for example at 68.98° and 75.66°. This corresponds well to the composition analysis which stated that there is only 1.13 wt% of titanium in Amang zircon sand.

The crystallite size was determined by using Scherrer formula as in Equation (6). The crystallite size of raw Amang zircon sand at peak 26.98° was determined to be 71.13 nm.

$$D_p = \frac{0.94\lambda}{\beta cos\theta} \quad (6)$$

where Dp is the average crystallite size, β is line broadening in radians (FWHM), θ is Bragg angle and λ is X-Ray wavelength.

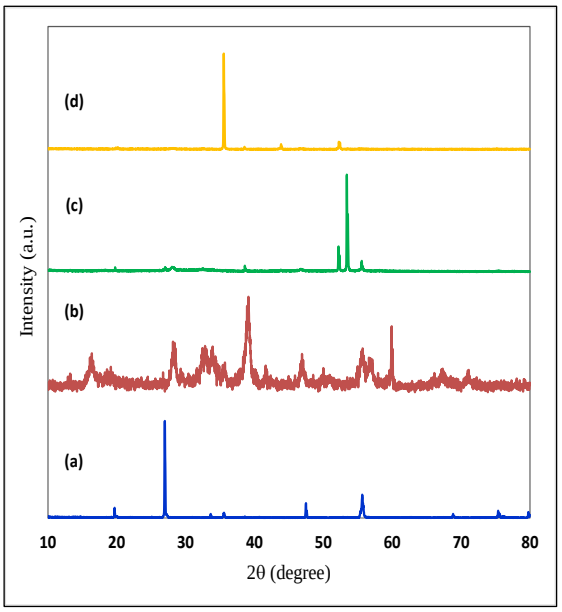


Figure 2. Diffraction pattern of (a) raw Amang zircon sand, (b) thermal treatment, (c) water leaching, and (d) acid leaching

XRD analysis of zircon after alkali fusion and thermal treatment was done by using the optimal ratio of NaOH to zircon sand which is 1.2 NaOH/$ZrSiO_4$. Based on the XRD pattern of thermal decomposition after the fusion of NaOH with zircon, the highest peak at 39.16° is due to the high composition of $Na_2ZrO_3$ with the crystallite size of 15.32 nm. This is also recorded by Da Silva *et al.* (2012). $Na_2SiO_3$ is also detected in some smaller peaks for example at peaks 28.16° and 47.06° alongside unreacted zircon at 28.08° (ICDD 00-036-0420). The presence of $Na_2ZrO_3$ and $Na_2SiO_3$ is in accordance with Equation (2) where two phases coexist after the thermal treatment. This proves that NaOH has successfully decomposed $ZrO_2$ and $SiO_2$ in the zircon sand and thus produced the water-soluble sodium silicate and water-insoluble sodium zirconate at the designated thermal temperatures. The usage of NaOH reduced the sintering temperature in which makes it a good decomposition agent compared to $CaCO_3$ and $Na_2CO_3$ (Sun *et al.*, 2019). The selected holding time of 1 and 2 hours are based on the commercially used holding time in the industry and it also help to boost the zircon decomposition (Liu *et al.*, 2016).

The water soluble $Na_2SiO_3$ and unreacted NaOH can be removed via the water leaching process. Based on the XRD pattern after water leaching, zirconium is still the major component that can be detected in almost every peak especially at the highest peak 55.58°. A small amount of $Na_2O$ can be found alongside with $ZrO_2$ and $SiO_2$ at 28.00° and 28.30°, respectively (ICDD 00-001-0791). The majority of sodium was removed after a series of washing. However, it is worth to note that the removal of sodium silicate and unreacted NaOH can be increased by mechanical stirring during the water leaching process. Thus, decreasing the excess Na+ that will then be reflected in the diffraction pattern.

The highest peak in the diffraction pattern of acid leaching treatment was recorded at 35.54° where a high presence of zirconium was detected (ICDD 00-002-0733). The crystallite size is 37.57 nm which is a good indication. According to Manivasakan *et al.* (2011), $ZrO_2$ nanoceramic with crystallite size of less than 100 nm exhibits great mechanical toughness and superplastic behaviour. Besides, a smaller crystallite size will result in a higher efficiency during a chemical reaction. A low amount of silicon was also detected as suggested in the XRF analysis in Table 1. At 43.86°, zirconium and silicon are detected. A small trace of unreacted zircon and sodium can also be found in some diffraction peaks. This is because the water insoluble $Na_2ZrO_3$ reacts with HCl based on Equation (5). Hence, excess sodium is observed, and formation of silicone gel can be seen. Other impurities such as titanium (Ti), yttrium (Y) and iron (Fe) were not detected. This might be because the composition is very small as shown in Table 1.

### *C. Particle Size Distribution*

The particle size distribution analysis was shown in Figure 3 and Table 2. The value of particle width distribution was obtained by using Equation (7):

$$S_w = \frac{2.56}{log\left(\frac{D_{90}}{D_{10}}\right)} \quad (7)$$

According to Subuki *et al.* (2020), the optimum value of a particle width distribution ($S_w$) was denoted to be less than 2 or greater than 7. $S_w$ smaller than 2 indicates a very broad distribution while a $S_w$ greater than 7 indicates a very narrow distribution. Based on the data obtained, the particles were in broad distributions except for raw Amang zircon which is detected to be at 9.47 which is higher than 7. This means that the raw Amang zircon has a very narrow distribution. According to Manivasakan *et al.* (2011), zirconia with uniform shape and narrow distribution is required in the development of functional ceramics.

The average particle size ($D_{50}$) of raw Amang zircon sand is determined to be 384.17 µm. This particle size is deemed to be slightly bigger. According to literature, a smaller particle size will increase the rate of reaction and increase the decomposition of zircon by increasing the contact area between reactants (Liu *et al.*, 2016). It is advisable to mill the raw Amang zircon sand into a smaller particle size for industrial sintering in order to increase the zirconium recovery. Conversely, the particle size should be bigger than 95 µm to control the formation of sodium silicate. This will reduce the excess sodium and silicon in the frit. It is interesting to note that milling process will also influence the phase transformation.

The particle size was greatly reduced to 204.09 µm after the thermal treatment, which resulted in a higher specific surface area at 0.227 $m^2/g$. This suggests that the particle size was reduced during the fusion in the furnace under a high temperature. The shrinkage occurred due to the reduction of volume fraction from the reaction of molten NaOH with zircon on the particle surface in Equation (1). However, the particle size after water leaching and acid reaching increased to 312.40 µm and 369.09 µm, respectively. According to Rauta *et al.* (2012), the increase of particle size is due to the partial removal of Fe and Na from the solid sodium zirconate. Besides, it also indicates that the sample is highly aggregated after the leaching process. This issue can be resolved by ball milling process.

The specific surface area (SSA) after acid leaching is reduced to 0.068 $m^2/g$. It is better to have a higher specific surface area since it will increase the chemical reaction and adsorption. The specific surface area decreased because the particle size increased from the aggregation. This is because specific surface area is highly in influence to the particle size. A greater particle size will affect the specific surface area by reducing the exposed surface. However, specific surface area can be increased by increasing the porosity (Jin *et al.*, 2016). This will also increase the strength as the thermal shock resistance increased. Thus, cracking can be avoided and the efficiency is increased.

After the acid leaching process, zirconium oxychloride which is the main raw materials of zirconium based compound has a particle width distribution that is almost the same as the commercially available zirconia which is at 2.49 (Subuki *et al.,* 2020). These findings show that it is possible to use Amang zircon sand as an inexpensive precursor to synthesis zirconia in a large scale production. This is due to the fact that zirconium oxychloride could be further processed into a highly valued yttria-stabilised zirconia (YSZ) by using coprecipitation method (Obal *et al.*, 2012).

Table 2. Parameters of particle size distribution

| **Specification** | **Particle Size µm** | | | **Particle width distribution ($S_w$)** | **Specific surface area ($m^2/g$)** |
|---|---|---|---|---|---|
| | **$D_{10}$** | **$D_{50}$** | **$D_{90}$** | | |
| Raw Amang Zircon | 281.76 | 384.17 | 524.99 | 9.47 | 0.016 |
| Thermal treatment | 11.93 | 204.09 | 579.82 | 1.52 | 0.227 |
| Water leaching | 24.24 | 312.40 | 609.32 | 1.83 | 0.131 |
| Acid leaching | 47.25 | 369.09 | 539.37 | 2.42 | 0.068 |

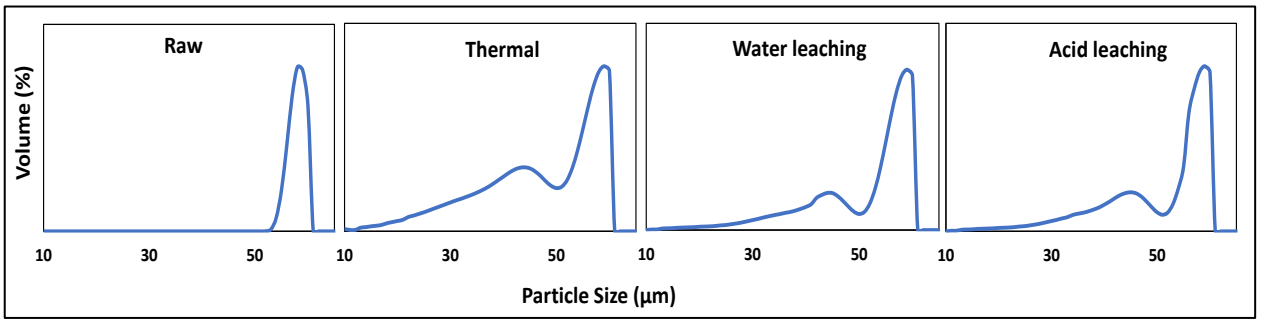


Figure 3. Particle size distribution of Amang zircon sand

## IV. CONCLUSION

A high zirconium composition is achieved from Amang zircon sand using alkali fusion method with sodium hydroxide in varied ratio of 1.2, 1.3 and 1.5 $NaOH/ZrSiO_4$. Based on the XRF analysis, XRD pattern and particle size analysis of the synthesised samples, the optimum ratio is determined to be 1.2 $NaOH/ZrSiO_4$ as it has the lowest silicon impurities with a high yield of zirconium. This shows that the impurities in Amang zircon sand can be reduced greatly. Lower impurity is important in zirconia in order to reduce the chance of cracking and maximising the efficiency. Besides that, zirconium oxychloride that was obtained after acid leaching treatment can be used as an inexpensive precursor for a stabilised zirconia using coprecipitation method with ammonium hydroxide. The zirconium composition can be further increased during the calcination of zirconia. Hence, the synthesised zirconium using Amang zircon sand from Amang Onn Sdn. Bhd. was successful.

## V. ACKNOWLEDGEMENT

The authors would like to thank for the financial support given under the Fundamental Research Grant Scheme (FRGS, 600-RMI/FRGS 5/3 (457/2019) from Universiti Teknologi MARA (UiTM) Shah Alam, Malaysia and Amang Onn Sdn. Bhd., Kampar, Perak mineral company for providing the raw Amang zircon sand for this research.

## VI. REFERENCES

Abdel-Rehim, AM 2005, 'A new technique for extracting zirconium form Egyptian zircon concentrate', International Journal of Mineral Processing, vol. 76, no. 4, pp. 234–243. doi: 10.1016/j.minpro.2005.02.004.

Abdelkader, AM, Daher, A & El-Kashef, E 2008, 'Novel decomposition method for zircon', Journal of Alloys and Compounds, vol. 460, no. 1–2, pp. 577–580. doi: 10.1016/j.jallcom.2007.06.032.

Abdelkareem, A 2019, 'New extraction technique of zirconium and hafnium from zircon mineral', Arab Journal of Nuclear Sciences and Applications, vol. 52, no. 2, pp. 201–208. doi: 10.21608/ajnsa.2019.3052.1066.

Abdullah, M. *et al.* 2022, 'The impact of unregulated industrial tin-tailing processing in Malaysia : Past , present and way forward', Resources Policy, vol. 78(December 2020), p. 102864. doi: 10.1016/j.resourpol.2022.102864.

Atkinson, I, Mocioiu, OC & Anghel, EM 2021, 'Original article A study of zircon crystallization, structure, and chemical resistance relationships in ZrO 2 containing ceramic glazes', *Boletín de la Sociedad Española de Cerámica y Vidrio*, pp. 1–9. doi: 10.1016/j.bsecv.2021.07.002.

Attallah, MF, Hilal, MA & Moussa, SI 2017, 'Quantification of some elements of nuclear and industrial interest from zircon mineral using neutron activation analysis and passive gamma-ray spectroscopy', Applied Radiation and Isotopes, vol. 128(July), pp. 224–230. doi: 10.1016/j.apradiso.2017.07.018.

Azreen, NM *et al.* 2018, 'Radiation shielding of ultra-high-performance concrete with silica sand, amang and lead glass', Construction and Building Materials, vol. 172, pp.

370–377. doi: 10.1016/j.conbuildmat.2018.03.243.

El Barawy, KA, El Tawil, SZ & Francis, AA 2000, 'Alkali fusion of zircon sand', Transactions of the Institutions of Mining and Metallurgy, Section C: Mineral Processing and Extractive Metallurgy, vol. 109(JAN./APR.), pp. 49–56. doi: 10.1179/mpm.2000.109.1.49.

Biswas, RK *et al.* 2010, 'A novel method for processing of Bangladeshi zircon: Part I: Baking, and fusion with NaOH', Hydrometallurgy, vol. 103, no. 1–4, pp. 124–129. doi: 10.1016/j.hydromet.2010.03.009.

Chen, L & Bonaccurso, E 2014, 'Effects of surface wettability and liquid viscosity on the dynamic wetting of individual drops', Physical Review E - Statistical, Nonlinear, and Soft Matter Physics, vol. 90, no. 2. doi: 10.1103/PhysRevE.90.022401.

Daou, EE 2014, 'The Zirconia Ceramic: Strengths and Weaknesses', The Open Dentistry Journal, vol. 8, no. 1, pp. 33–42. doi: 10.2174/1874210601408010033.

Das, K & Bandyopadhyay, TK 2004, 'Synthesis and characterization of zirconium carbide-reinforced iron-based composite', Materials Science and Engineering A, vol. 379, no. 1–2, pp. 83–91. doi: 10.1016/j.msea.2003.12.022.

Ebrahimi, M, Hamidi, AG & Pourabdoli, M 2022, 'Utilization of Na2CO3 for intermediate phase formation in vanadium-zircon pigment synthesis', Materials Chemistry and Physics, vol. 281(December 2021), p. 125875. doi: 10.1016/j.matchemphys.2022.125875.

Gauna, MR *et al.* 2015, 'Monoclinic-tetragonal zirconia quantification of commercial nanopowder mixtures by XRD and DTA', Ceramics - Silikaty, vol. 50, no. 4, pp. 318–325.

Genoveva, GR *et al.* 2007, 'The Influence of Agitation Speed on the Morphology and Size Particle Synthesis of Zr(HPO4)2·H2O from Mexican Sand', Journal of Minerals and Materials Characterization and Engineering, vol. 06, no. 01, pp. 39–51. doi: 10.4236/jmmce.2007.61004.

Hamzah, Z, Ahmad, M & Saat, A 2009, 'Determination of heavy minerals in "Amang" from kampung gajah ex-mining area', The Malaysian Journal of Analytical Sciences, vol. 13, no. 2, pp. 194–203.

Hidalgo, J *et al.* 2013, 'Effect of a binder system on the low-pressure powder injection moulding of water-soluble zircon feedstocks', Journal of the European Ceramic Society, vol. 33, no. 15–16, pp. 3185–3194. doi: 10.1016/j.jeurceramsoc.2013.06.027.

Ismail, B *et al.* 2001, 'Radiological impacts of the amang processing industry on neighbouring residents', Applied Radiation and Isotopes, vol. 54, no. 3, pp. 393–397. doi: 10.1016/S0969-8043(00)00106-8.

Jin, X *et al.* 2016, 'Effects of porosity and pore size on mechanical and thermal properties as well as thermal shock fracture resistance of porous ZrB2-SiC ceramics', Ceramics International, vol. 42, no. 7, pp. 9051–9057. doi: 10.1016/j.ceramint.2016.02.164.

Keiteb, AS *et al.* 2017, 'Structural and optical properties of Zirconia nanoparticles synthesized by thermal treatment method', Nanomaterialsaterials, vol. 10, no. 4, p. 402. doi: 10.3390/ma10040402.

Kittiauchawal, T *et al.* 2012, 'The effect of heat treatment on crystal structure in zircon monitored by ESR and XRD', Procedia Engineering, vol. 32, pp. 706–713. doi: 10.1016/j.proeng.2012.02.001.

Kumar, P *et al.* 2015, 'Enhancement of thermal shock resistance of reaction sintered mullite-zirconia composites in the presence of lanthanum oxide', Materials Characterization, vol. 101, pp. 34–39. doi: 10.1016/j.matchar.2015.01.004.

Li, J *et al.* 2022, 'High-efficiency preparation of zircon ceramics using borosilicate glass as sintering additive', Ceramics International, vol. 48, no. 15, pp. 22506–22515. doi: 10.1016/j.ceramint.2022.04.270.

Liu, J *et al.* 2016, 'Controlling the formation of Na2ZrSiO5 in alkali fusion process for zirconium oxychloride production', Advanced Powder Technology, vol. 27, no. 1, pp. 1–8. doi: 10.1016/j.apt.2015.08.005.

Liu, R *et al.* 2014, 'Analysis of water leaching and transition processes in zirconium oxychloride octahydrate production', Ceramics International, vol. 40(1 PART B), pp. 1431–1438. doi: 10.1016/j.ceramint.2013.07.026.

Mohammed, NA & Daher, AM 2002, 'Preparation of high-purity zirconia from Egyptian zircon: An anion-exchange purification process', Hydrometallurgy, vol. 65, no. 2–3, pp. 103–107. doi: 10.1016/S0304-386X(02)00042-7.

Morfino, A *et al.* 2022, 'Life cycle assessment comparison between zircon and alumina sand applied to ceramic tiles', Cleaner Engineering and Technology, vol. 6, p. 100359. doi: 10.1016/j.clet.2021.100359.

Murti, CFK *et al.* 2019, 'Particle size analysis of the synthesised zro2 from natural zircon sand with variation of ph deposition using alkali fusion-coprecipitation method', Materials Science Forum, vol. 966 MSF, pp. 89–94. doi: 10.4028/www.scientific.net/MSF.966.89.

Musyarofah *et al.* 2019, 'Synthesis of high-purity zircon, zirconia, and silica nanopowders from local zircon sand',

Ceramics International, vol. 45, no. 6, pp. 6639–6647. doi: 10.1016/j.ceramint.2018.12.152.

Obal, K *et al.* 2012, 'Modification of yttria-doped tetragonal zirconia polycrystal ceramics', International Journal of Electrochemical Science, vol. 7, no. 8, pp. 6831–6845.

Pawłowski, L, Blanchart, P & Blanchart, P 2018, 'Extraction, Properties and Applications of Zirconia', Industrial Chemistry of Oxides for Emerging Applications, pp. 165–209. doi: 10.1002/9781119424079.ch4.

Rauta, PR *et al.* 2012, 'Phase transformation of ZrO 2 nanoparticles produced from zircon', Phase Transitions, vol. 85, no. 1–2, pp. 13–26. doi: 10.1080/01411594.2011.619698.

Sanusi, MSM *et al.* 2021, 'Ecotoxicology and Environmental Safety Radiological hazard associated with amang processing industry in Peninsular Malaysia and its environmental impacts', Ecotoxicology and Environmental Safety, vol. 208, p. 111727. doi: 10.1016/j.ecoenv.2020.111727.

Septawendar, R *et al.* 2016, 'A Low-Cost, Facile Method on Production of Nano Zirconia and Silica from Local Zircon in a Large Scale Using a Sodium Carbonate Sintering Technology', Journal of The Australian Ceramic Society, vol. 52, no. 2, pp. 92–102.

Shi, F *et al.* 2012, 'Fabrication of well-dispersive yttrium-stabilized cubic zirconia nanoparticles via vapor phase hydrolysis', Progress in Natural Science: Materials International, vol. 22, no. 1, pp. 15–20. doi: 10.1016/j.pnsc.2011.12.003.

Da Silva, RJF, Dutra, AJB & Afonso, JC 2012, 'Alkali fusion followed by a two-step leaching of a Brazilian zircon concentrate', Hydrometallurgy, vol. 117–118, pp. 93–100. doi: 10.1016/j.hydromet.2012.02.011.

Subuki, I *et al.* 2020, 'Study of the Synthesis of Zirconia Powder from Zircon Sand obtained from Zircon Minerals Malaysia by Caustic Fusion Method', Indonesian Journal of Chemistry, vol. 20, no. 4, p. 782. doi: 10.22146/ijc.43936.

Sun, H qian *et al.* 2019, 'Decomposition kinetics of zircon sand in NaOH sub-molten salt solution', Transactions of Nonferrous Metals Society of China (English Edition), vol. 29, no. 9, pp. 1948–1955. doi: 10.1016/S1003-6326(19)65102-2.

Van Tuyen, N *et al.* 2007, 'Preparation of High Quality Zirconium Oxychloride From Zircon of Vietnam', pp. 286–291.

Yang, X *et al.* 2021, 'Progress in Nuclear Energy Rapid preparation of zirconia / zircon composites ceramics by microwave method : Experiment and first-principle investigation', Progress in Nuclear Energy, vol. 139(June), p. 103839. doi: 10.1016/j.pnucene.2021.103839.